

Raman spectroscopy study of rotated double-layer graphene: misorientation angle dependence of electronic structure

*Kwanpyo Kim^{1,2,3}, Sinisa Coh^{1,3}, Liang Z. Tan^{1,3}, William Regan^{1,3}, Jong Min Yuk^{1,3,4}, Eric Chatterjee¹,
M. F. Crommie^{1,2,3}, Marvin L. Cohen^{1,2,3}, Steven G. Louie^{1,3}, and A. Zettl^{1,2,3}*

¹Department of Physics and ²Center of Integrated Nanomechanical Systems, University of California at Berkeley, ³Materials Sciences Division, Lawrence Berkeley National Laboratory, Berkeley, CA 94720, U.S.A. and ⁴Department of Materials Science and Engineering, KAIST, Daejeon 305-701, Korea.

- Contents -

- 1. Sample preparation**
- 2. TEM analysis of single layer graphene**
- 3. TEM analysis of rotated double-layer graphene**
- 4. Raman spectroscopy**
- 5. Details of tight-binding calculation**
- Supplementary Figures S1-S6**
- References**

1. Sample preparation

Rotated double-layer graphene samples are fabricated by stacking two layers of chemical vapor deposition (CVD)-grown graphene on Quantifoil holey carbon TEM grids. After CVD graphene synthesis [S1], we perform a direct transfer method for transferring CVD graphene to TEM grids [S2]. Then we repeat the graphene transfer process to obtain the double-layer samples [S2,S3]. Supplementary Figure S1 show the optical and low-magnification TEM images of a sample. The TEM grid has an array of holes with 2 μm diameters.

2. TEM analysis of single layer graphene

Supplementary Figure S2 shows the TEM image and diffraction analysis of single-layer graphene. Our CVD-grown graphene is generally clean with some minor residues (Fig. S2a). Diffraction pattern shows a hexagonal spot pattern (Fig. S2b) and inner (0-110) and outer (1-210) spot intensities show 1:1 ratio (Fig. S2c,d). This confirms that the region is composed of single-layer graphene [S4,S5]. An electron beam size of $\sim 1 \mu\text{m}$ is used for diffraction acquisition.

3. TEM analysis of rotated double-layer graphene

With TEM imaging and diffraction, we analyze the relative rotation angles between stacked graphene layers. We check whether the graphene has tilt grain boundaries [S4] or local folds [S6], which prevents us from assigning well-defined rotation angles. We also minimize the electron beam damage to graphene samples by performing only low magnification imaging and diffraction with low electron beam intensity. Supplementary Figure S3 show the TEM image and diffraction analysis of rotated double-layer graphene. Double-layer graphene has scattered dark regions, which are most likely carbon residues trapped between two layers (Fig. S3a). These dark regions can be used to quickly distinguish double-layer from single-layer graphene regions in our samples. If the double layer graphene has no tilt grain boundary or fold, diffraction patterns exhibit two sets of hexagonal patterns from two rotated graphene crystals as shown in Fig. S3b. Analysis shows that the two rotated patterns have the similar intensities and maintain the single-layer signature, respectively. This confirms that the region is composed of two stacked, rotated single-crystal graphene layers (Fig. S3c,d). Misorientation angles can be defined between zero and thirty degrees due to graphene hexagonal symmetry (Fig. S3e). Regular TEM imaging and diffraction acquisition were performed in a JEOL 2010 microscope at 100 kV. Atomic resolution TEM images are also acquired at 80 kV with a TEAM 0.5 microscope, at the National Center for Electron Microscopy, Lawrence Berkeley National Laboratory after Raman measurements.

4. Raman spectroscopy

All the Raman spectroscopy measurements were performed with a Renishaw inVia Raman microscope in ambient pressure at room temperature. 633 nm (1.96 eV), 514 nm (2.41 eV), and 488 nm (2.54 eV) laser wavelengths (energies) are used for measurements. A laser beam size of $\sim 1 \mu\text{m}$ with $\times 100$ objective lens is used. All the measurements were performed with low power ($< 0.2 \text{ mW}$) to prevent a heating effect on the suspended graphene samples.

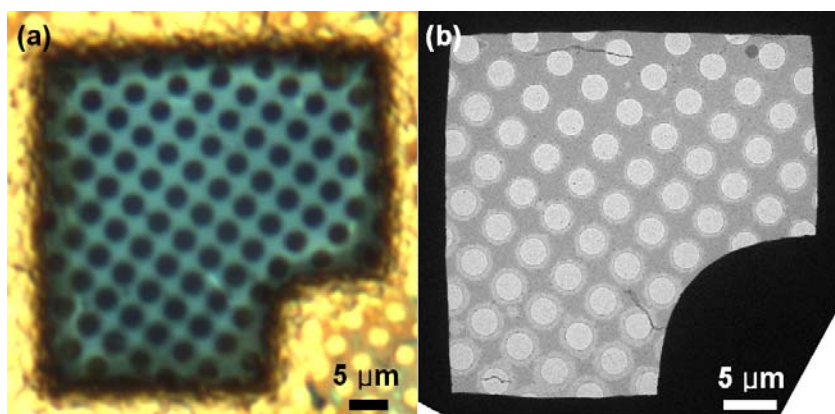
5. Details of tight-binding calculation

The Raman intensities are calculated from the tight-binding band structure and electronic wavefunctions by summing over terms in a perturbation expansion in the electron-photon and electron-phonon interactions. For the G peak we need to expand to third order, since it involves only one electron-phonon and two electron-photon interactions, while for 2D peak we need to expand to fourth order since it involves two phonon processes.

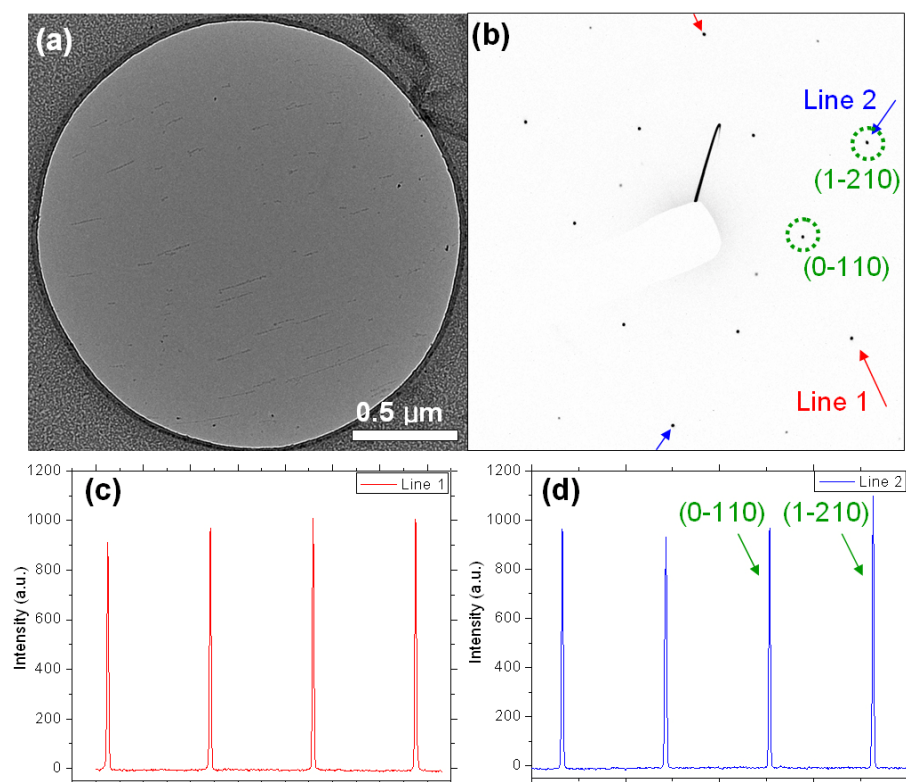
The primitive unit cell of a rotated double-layer graphene is much larger than that of a single layer graphene having only two carbon atoms (smallest unit cells are 7, 13, 19, and 31 times larger in size). For this reason, the BZ of a rotated double-layer graphene is reduced in size and any given \mathbf{k} vector in the rotated double-layer BZ corresponds to a set of $\mathbf{k} + \mathbf{G}_i$ vectors in the corresponding top and bottom BZ. Here \mathbf{G}_i is a set of reciprocal vectors of the rotated double layer BZ chosen so that the $\mathbf{k} + \mathbf{G}_i$ vectors for all \mathbf{k} cover both the top and bottom monolayer reciprocal space exactly once.

As explained in the main manuscript, we assume that the phonon band structure of the rotated graphene layers is identical to that of monolayer graphene, and we simply fold it from single-layer BZ into a double-layer BZ. We use computed single-layer phonon bandstructure from Ref. [S7]. Furthermore, we approximate phonon eigenvectors at an arbitrary point near K (or K') with that at K (or K') point.

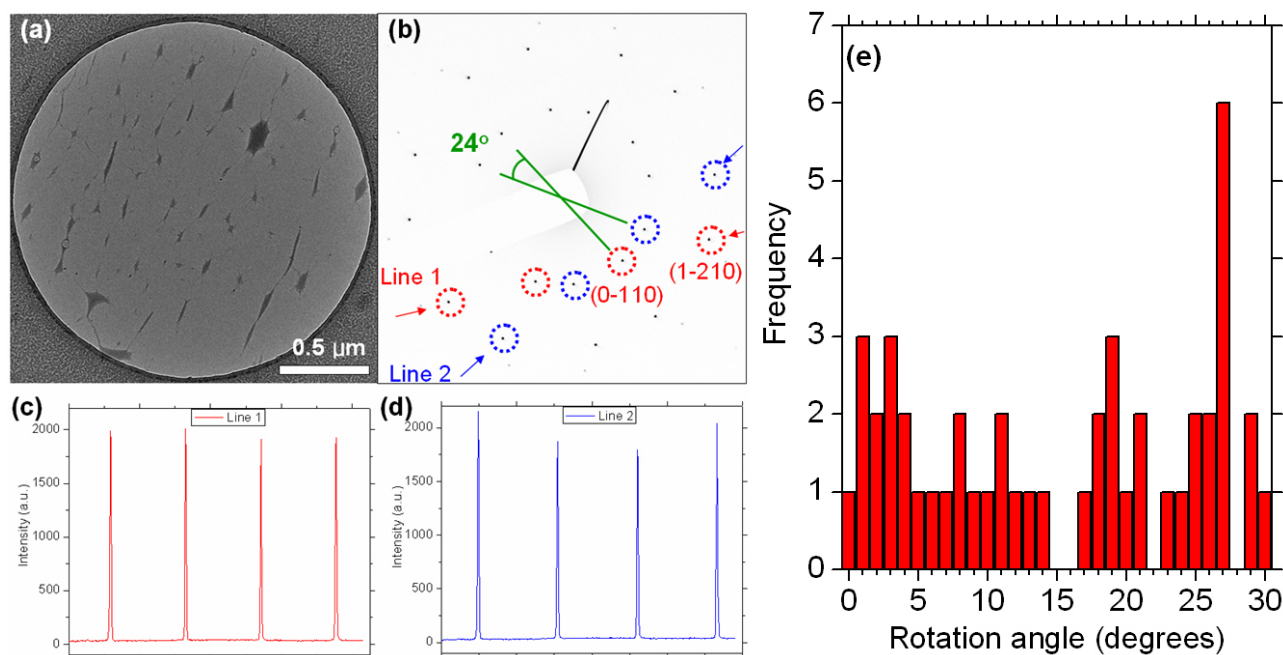
In order to further elucidate the origin of the 2D Raman features, we compare our Raman spectrum calculations with two different fictitious calculations. In the first, all electronic eigenenergies in the Raman intensity sum are replaced by the corresponding values in monolayer graphene, using the electronic wavefunctions of the rotated graphene layers. In the second, the values of the electronic wavefunctions in the Raman intensity sum are instead that of the graphene monolayer, while the eigenenergies are that of the rotated graphene layers.



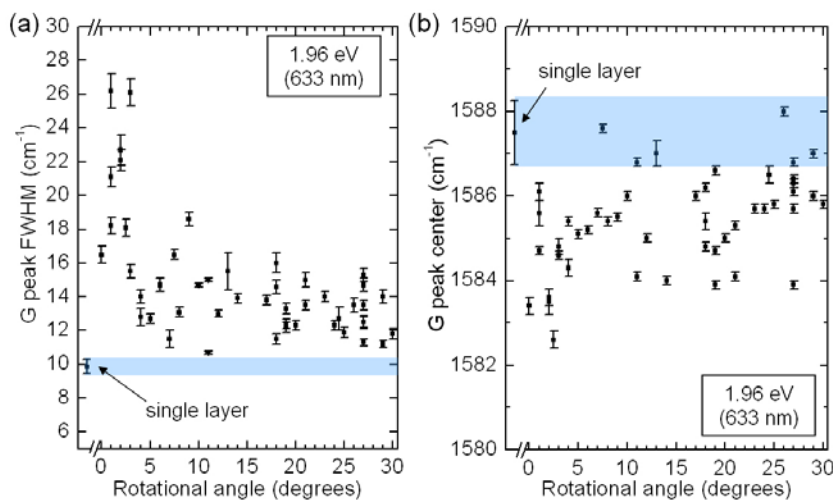
Supplementary Figure S1. Double-layer graphene samples on a TEM grid. (a) Optical image of a sample. (b) Low-magnification TEM image of the same regions of the sample.



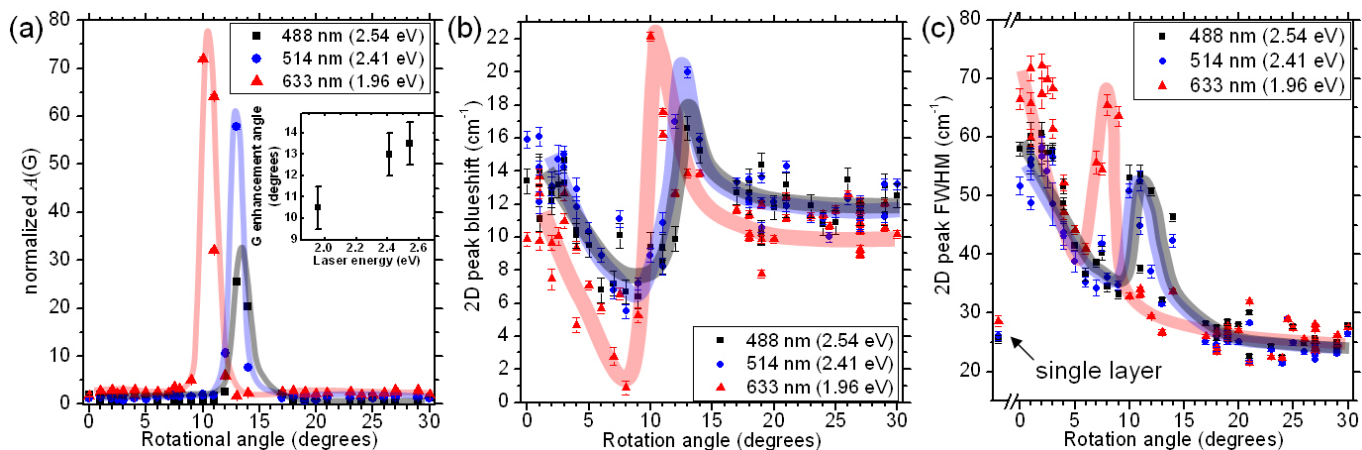
Supplementary Figure S2. TEM imaging and diffraction of single layer graphene. (a) TEM image of the suspended monolayer CVD graphene. The diameter of the hole is 2 μm . (b) Diffraction pattern of the center region in the hole. The diffraction shows the hexagonal pattern. The arrows indicate the lines for intensity scan for Fig. c and d. The diffraction is acquired with about 1 μm e-beam size. (c) Line intensity of line 1. The intensities of inner and outer spot are comparable, showing that the graphene is monolayer. (d) Line intensity of line 2.



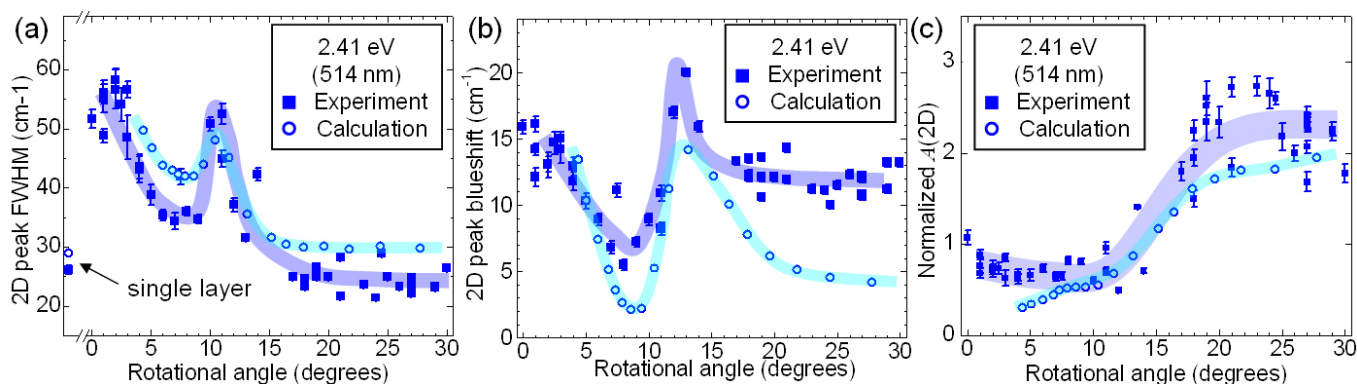
Supplementary Figure S3. TEM imaging and diffraction of double layer graphene. (a) TEM image of double layer graphene. (b) Diffraction pattern of the graphene sample shown in Fig a. It shows 24 degree rotation. The arrows indicate the lines for intensity scan for Fig. c and d. The diffraction is acquired with about 1 μm e-beam size. (c) Line intensity of line 1. (d) Line intensity of line 2. (e) Histogram of rotation angles in the studied double-layer graphene samples.



Supplementary Figure 4. Rotational angle dependence of Graphene G peak FWHM and center location measured with 633 nm laser wavelength. (a) Rotated double-layer graphene G peak full-width half-maximum (FWHM). The blue horizontal area represents the value from single layer graphene. (b) Rotated double-layer graphene G peak center location. The blue horizontal area represents the value from single layer graphene.



Supplementary Figure S5. Experimental Raman data on rotated double-layer graphene with different laser wavelengths. The general features in the data are shifted to higher rotational angles with higher laser energies. (a) G peak intensity depending on the rotation angle. Intensities were normalized to the single-layer value for each laser wavelength. The inset shows the laser energy dependence of rotational angles with G enhancement. (b) 2D peak blue-shift depending on the rotation angle compared to single-layer graphene values. (c) Graphene 2D peak FWHM depending on the rotation angle.



Supplementary Figure S6. Rotational angle dependence of Raman 2D peak with 514 nm laser wavelength (2.41 eV). (a) Rotated double-layer graphene 2D peak FWHM. The squares and circles are the experimental and theoretical calculation values. The blue (experiment) and bright blue (calculation) lines are guides to the eye. (b) Rotated double-layer graphene 2D peak blue-shift with respect to the value from single layer graphene. (c) Integral intensity of 2D peak. Experimental and calculation values are normalized to the single-layer value.

References

- [S1] X. Li *et al.*, *Science* **324**, 1312-1314 (2009).
- [S2] W. Regan *et al.*, *Appl. Phys. Lett.* **96**, 113102 (2010).
- [S3] J. M. Yuk *et al.*, *Nano Lett.* **11**, 3290-3294 (2011).
- [S4] K. Kim *et al.*, *ACS Nano* **5**, 2142-2146 (2011).
- [S5] J. C. Meyer *et al.*, *Nature* **446**, 60-63 (2007).
- [S6] K. Kim *et al.*, *Phys. Rev. B* **83**, 245433 (2011).
- [S7] P. Venezuela *et al.*, *Phys. Rev. B* **84**, 035433 (2011).